Longitudinal Study of Exposure to Radio Frequencies at Population Scale

Yanis Boussad, Xi Leslie Chen, Arnaud Legout, Augustin Chaintreau, Walid Dabbous

Longitudinal Study of Exposure to Radio Frequencies at Population Scale

Yanis Boussad[a], Xi (Leslie) Chen[b], Arnaud Legout[a,*], Augustin Chaintreau[b], Walid Dabbous[a]

[a] *Université Côte d'Azur, Inria. Sophia Antipolis, 06902, France*
[b] *Columbia University. New York, NY 10027, USA*

Abstract

Evaluating population-scale exposure to the radio frequencies (RF) used in wireless telecommunication technologies is important for conducting sound epidemiological studies on the health impacts of these RF [1, 2]. Numerous studies have reported population exposure, but have used very small population samples. In this context, the real exposure of the population to RF remains subject to controversy [3, 4, 5, 6]. Here, to the best of our knowledge, we report the largest crowd-based measurement of population exposure to RF produced by cellular antennas, Wi-Fi access points, and Bluetooth devices for 254,410 unique users in 13 countries from January 2017 to December 2020. All measurements were obtained from the ElectroSmart Android app [7], and we applied a thorough methodology to clean and consolidate the measurements. We show that total exposure has been multiplied by 2.3 in the four-year period considered, with Wi-Fi as the largest contributor. The cellular exposure levels are orders of magnitude lower than the regulation limits and not significantly impacted by national regulation policies. Therefore, the mere comparison of exposure levels to regulation limits is a poor way to describe the real evolution of exposure. The population tends to be more exposed at home; for half of the study subjects, personal Wi-Fi routers and Bluetooth devices contributed to more than 50% of their total exposure. We make our dataset publicly available to provide a starting point for sound epidemiological studies on the health impacts of RF, and for other types of studies interested in population exposure to RF or the usage of wireless communication technologies.

Keywords: radiofrequency, population exposure, crowdsource, personal measurements, large-scale

1. Introduction

The long-term impact of radio frequencies on health is a long-standing scientific question that is well illustrated by the classification of radio frequencies as a Group 2B carcinogen by the WHO [8]. This classification means that *there is some evidence that it can cause cancer in humans but at present it is far from conclusive*[9]. Total exposure to various sources of radio frequencies is considered a critical factor for mitigating health hazards, but in the wild, this exposure varies greatly with time and among individuals. Environmental and behavioral factors play a role, as previous assessments have shown[10, 11, 12, 13, 14, 15, 16, 17, 18, 19, 20, 21, 22, 23, 24, 25, 26], limiting the generalizability of results obtained from small study-groups or sparsely instrumented measurements. We present here the first longitudinal analysis of exposure events on a large subject population; results span four years, from approximately a quarter-million unique subjects in 13 countries across Europe, the Americas, Asia, and Australia. The scale of our study allows us to offer the first generalizable findings on critical epidemiological questions regard-

*Corresponding author
Email address: arnaud.legout@inria.fr (Arnaud Legout)

ing the growth of radio exposure worldwide and the respective contributions of different technologies to this growth. We also consider the effectiveness of regulation and some of the factors within an individual's control that affect exposure. Beyond these advances, the release of our data (in a form rendering users unidentifiable) can facilitate large-scale epidemiological studies on the impact of radio frequencies. The data were collected using the crowdsourcing Android app Electrosmart [7] that we developed to instrument a smartphone's baseband and report Received Signal Strength Indicators (RSSI) for radio frequencies received from cellular infrastructures, Wi-Fi access points, and Bluetooth devices. Our dataset includes the exposure of 254,410 unique persons from January 2017 to December 2020.

2. Materials and Methods

This study relies heavily on the quality of the data we collected. In this section, we present our data collection methodology, the dataset we collected, and the cleaning we applied to this dataset.

2.1. Data collection

2.1.1. The ElectroSmart measurement app

ElectroSmart [7] is an Android consumer app we designed to measure the power that a given smartphone receives from Wi-Fi access points, Bluetooth devices, and cell towers. To reach a large audience, we put a great deal of effort into the user experience, designing ElectroSmart to be an easy-to-use tool that offers users transparent information on their exposure to radio frequencies. ElectroSmart can be installed on any Android smartphone running Android 4.1 or later. The app was first launched in August 2016, and as of May 18$^{\text{th}}$, 2021, it had 900,000 downloads and 190,000 active users.

ElectroSmart performs an *exposure scan* every 20 minutes when used in the background. All scans are periodically collected on our servers. Below, we explain how an exposure scan works and describe the information it collects. We discuss user consent and privacy protection in the following section. A scan performs the following actions.

- It creates a timestamp with the local time in UTC. This is a slight approximation as signals might not be measured at exactly the same time in a given measurement scan. However, by considering a window of a few seconds, it is easy to attribute all measured signals to a given measurement scan and timestamp (we specifically discuss the case of Bluetooth in the section *Bluetooth scan synchronization*).
- It collects characteristics of the smartphone (brand and model) and its Android version.
- It measures the smartphone location in terms of latitude and longitude. Android provides this information by combining GPS, Wi-Fi access points, and cell tower information using a proprietary algorithm.
- It measures the *downlink* Received Signal Strength Indicator (RSSI) of all measurable Wi-Fi access points, Bluetooth devices, and cell towers (we discuss limitations below), along with several source-specific data.
  - For Wi-Fi access points, we collect the SSID, the BSSID, the frequency, and whether the user is connected to this access point.
  - For Bluetooth devices, we collect the device name, the device MAC address, and whether the user is bonded to this device.
  - For cell towers, we identify whether the cell is using a 2G, 3G, 4G, or CDMA/EVDO technology. We determine whether the cell is serving (that is, the user is currently connected to this cell), and we collect cell identification information, such as the Mobile Network Code (MNC), Mobile Country Code (MCC), or Cell ID (CID), to generate a unique identity for each cell tower.

2.1.2. Ethical and legal considerations

We submitted the study protocol to our institutional ethical committee (Inria COERLE [27]). They provided guidelines for respecting user privacy, consent, and data protection.

	WiFi	Bluetooth	Cellular (2G, 3G, 4G)
Max	-1	-1	-51
Min	-126	-150	-113

Table 1: **Valid range of the RSSI (in dBm) for each wireless protocol.**

ElectroSmart requires explicit user consent for all information collection. In particular, we are fully compliant with the European General Data Protection Regulation (GDPR) [28].

In addition, ElectroSmart is used anonymously by default, unless a user decides to provide an email address. The email address field is clearly identified as optional.

All scans are associated with a unique user ID. This user ID is randomly generated on our server at the app installation time. It is not linked to any unique smartphone or user information.

2.1.3. Limitations

We perform all scans with a vanilla version of Android using the regular Android API. That is, we do not have access to low-level data available from rooted smartphones or customized drivers. This approach is beneficial for targeting a large-scale audience, but it limits what we can measure, as elaborated below.

First, we only measure the downlink received by the measuring smartphone. Therefore, the contribution of the uplink to the exposure, that is, the emission of the measuring smartphone, is not considered in this study. Also, we do not measure the uplink of surrounding devices.

Second, the minimum and maximum measurable power for each wireless technology is capped by the Android API and the technology standards. We show in Table 1 the valid ranges of measurements for each technology. For example, if a smartphone is exposed to a higher power than the maximum measurable power, it will always report the maximum value presented in Table 1. We explain in *Dataset Cleaning* how we filter out-of-range scans.

Third, for 2G, 3G, and 4G, the RSSI is provided by the Android API as an *Arbitrary Strength Unit* (ASU), an integer value between 0 and 31. It is converted to dBm according to the formula: $\text{dBm} = \text{ASU} * 2 - 113$. For this reason, the granularity of the cellular RSSI is 2 dB.

Fourth, each wireless technology comes with some additional limitations. Bluetooth sources can only be measured when they are *discoverable*. Wi-Fi sources can only be measured when they are configured as access points, that is, the emitting power of the connected devices is not measured. Measurements of cellular sources suffer from several limitations. i) A smartphone with an active SIM card can only measure the RSSI from the operators declared in the SIM card. In practice, it is either the cellular operator that owns the SIM card (MNO), the cellular operator that is operating the cellular infrastructure for the virtual operator (MVNO), or the operators that partner with the MNO of the SIM card in foreign countries (Roaming). We explain in the Dataset Processing section how we mitigate this issue. ii) The measurement coverage is largely dependent on the version of Android and the cell phone maker. Indeed, the Android API can return the RSSI of the serving cell for all smartphones, but only the most recent versions of Android can also return the neighboring cells' RSSI. In addition, this API tends to be quite buggy due to the Android RIL (Radio Interface Layer, which is closed-source and vendor-specific. In particular, some smartphones return invalid RSSI measurements (outside of the range given in Table 1). We discuss in *Dataset Cleaning* how we identify and remove invalid measurements. iii) Smartphones periodically scan for cellular networks to ensure continuity of service. To speed up network scanning, smartphones follow priority rules that are defined by the network and stored in the SIM card. This means that a given smartphone may not scan for all the cellular Radio Access Technology (RAT), but instead, scan only high priority RATs. For example it may scan only 4G and 3G networks, excluding 2G. As a result, we expect the cellular scans not to include all the cellular generations in a single scan.

Last, the received power is measured using the Received Signal Strength Indicator (RSSI). Therefore, our measurements do not take into account the effective load of the wireless channel.

2.2. Dataset characteristics

In this study, we use all the exposure scans collected from January 2017 to December 2020 (4 years) representing 506,100 user profiles and 6,438 million measured RSSI.

We first clean this raw dataset as follows: i) we remove all measurements with invalid GPS coordinates, ii) we remove all measurements with invalid RSSI values, iii) we keep only measurements from the 13 countries with the largest number of measurements, iv) we remove all CDMA/EVDO measurements.

Then, we process the remaining measurements: v) we convert all timestamps to the local time of the country of origin, vi) we identify the Wi-Fi physical sources, vii) we attribute each Bluetooth measurement to an atomic scan. The following sections detail each of these seven steps.

2.2.1. Dataset cleaning

Invalid GPS coordinates removal. Background measurements are quite fast (typically a few seconds). There is usually not enough time to get a valid GPS coordinate from scratch, that is, when the GPS was not activated before the scan or when no prior information is cached to help the GPS converge faster to a location. However, location is a system-wide property, so if another app or the system has recently accessed the device location, we will benefit from this when we make the scan. Also, when the device is not power-constrained, we can allow more time to get a valid GPS location.

When a GPS coordinate cannot be retrieved in the ElectroSmart app, we set both the latitude and the longitude associated with a scan to either 0 or -1 depending on the root cause (in this paper, we do not exploit this root cause). As one of our goals is to explore the evolution of the exposure per country, we removed all scans with a GPS coordinate set to either 0 or -1. We removed 7.9% of the Wi-Fi measurements, 9% of the Bluetooth measurements, 18.2% of the 2G measurements, 19.8% of the 3G measurements, and 12.8% of the 4G measurements. Overall, we removed 11.2% of all the raw measurements by filtering out invalid GPS coordinates.

Invalid RSSI removal. The Android OS is an open-source software program that is common to all Android devices, but each smartphone manufacturer adapts it to their hardware by performing customization and developing drivers, all of which are proprietary. Therefore, each smartphone model can come with specific bugs [29]. This step focuses on the RSSI, which is produced by the proprietary Radio Interface Layer (RIL).

Fortunately, each wireless standard comes with a valid range for the RSSI value, as shown in Table 1. We can therefore easily filter out each measurement with an out-of-range RSSI value. We removed 0.07% of the Wi-Fi measurements, 0.04% of the Bluetooth measurements, 0.8% of the 2G measurements, 2.4% of the 3G measurements, and 14.1% of the 4G measurements. After this removal step, 85.9% of all the raw measurements remained.

In addition to the out-of-range values, we also observed in-range abnormal values for cellular measurements (2G, 3G, 4G). Abnormal values are in the valid range but tend to appear with higher frequency in the same *exposure scan*. The root cause of these abnormal values is hard to pinpoint as it most likely comes from bugs in the proprietary RIL. In particular, we observed that all smartphones with an Exynos [30] System on Chip (SoC)[1] have an abnormally high number of -51 dBm measurements: for all cellular measurements performed from smartphones with an Exynos SoC, the -51 dBm values represent 71% of all cellular measurements, whereas, they represent 1.91% for all smartphones running any SoC other than Exynos.

We found that the cells reporting abnormal values correspond to fake cells, that is, when the RIL reports a cell, but it does not correspond to a real measured cell. Indeed, when a smartphone connects to a cellular operator, it measures various performance indicators (including the RSSI), and connects to the cell with the best performance indicator; we call this cell the *serving cell*. All the other cells are called *neigh-*

[1]Most likely, the issue comes from the modem associated with the Exynos SoC, but we only have access to the SoC name from the Android API.

boring cells. We found that for 3G, the percentage of neighboring cells measured by smartphones with an Exynos SoC is 21.8% of all measured cells, whereas it is 2.7% for smartphones running any SoC other than Exynos. This is a clear indication that smartphones with an Exynos SoC report fake neighboring cells, at least for 3G.

Due to the bogus behavior of smartphones running an Exynos SoC, we decided to adopt a conservative strategy by removing all measurements (Wi-Fi, Bluetooth, 2G, 3G, 4G) performed by a smartphone with an Exynos SoC. Even if the issue does not concern Wi-Fi and Bluetooth, removing only cellular measurements (while keeping Wi-Fi and Bluetooth measurements) would have affected our discussion of personal exposure by changing the proportion of the sources of exposure. We removed 24.4% of the Wi-Fi measurements, 33.5% of the Bluetooth measurements, 7.9% of the 2G measurements, 40.6% of the 3G measurements, and 10.8% of the 4G measurements. After this removal step, 62.6% of all raw measurements remained.

For the sake of completeness, we note that we also observed an abnormally large number of measurements with a -113 dBm RSSI for 2G and, to a lesser extent, for 3G. We did not, however, find any correlation between these -113 dBm measurements and a specific SoC, device brand, or Android version. As dBm are in a logarithmic scale, and since we perform all our computations in Watt, which is in a linear scale, the impact of these measurements on the rest of this paper is negligible.

Included countries. ElectroSmart was released in August 2016 in two languages, English and French. We added Italian and German in March 2019, and Spanish and Portuguese in January 2020. France is the country with the largest number of measurements (36% of all measurements after removing invalid GPS and RSSI), followed by the USA (27.5%), Italy (7.9%), and Germany (4.6%).

We restricted this study to the 13 countries with the largest number of measurements. In addition to France, the USA, Italy, and Germany, we included (in order from the highest to the lowest number of measurements) Canada, the United Kingdom, Switzerland, Belgium, Spain, the Netherlands, India, Australia, and Brazil. Although Brazil accounts for only 0.5% of all measurements, this still represents 21.6 million measurements and 2668 unique users.

Altogether, the excluded countries represent 9.3% of all measurements. So, after this step, 56.8% of all raw measurements and 50.3% of all user profiles remained.

CDMA removal. The term CDMA refers to a large family of cellular protocols (cdmaOne, CDMA2000, EVDO) deployed mainly in North America. ElectroSmart can measure CDMA cells, but, apart from in the USA, we did not find CDMA measurements in any of the selected countries. In the USA, all CDMA measurements represent 0.95% of all cellular measurements (4G measurements represent 64% of all cellular measurements). As CDMA measurements are only used in the USA in our filtered dataset and represent a negligible fraction of all cellular measurements, we decided to remove all CDMA measurements from our dataset.

Cleaned dataset characteristics. In the rest of this paper, we will only refer to the cleaned dataset that resulted from the previous removal steps. This dataset contains 254,410 user profiles and 3,656 million measured RSSI. This represents 56.8% of all the measurements and 50.3% of all the profiles available in the raw dataset.

In this cleaned dataset, Wi-Fi represents 58.3% of all measured RSSI, Bluetooth 6.6%, 2G 10.5%, 3G 7.6%, and 4G 17%.

2.2.2. Dataset processing

Adapting to local time. All the raw measurements in the dataset are associated with a timestamp in UTC that corresponds to the instant the corresponding signal was detected. In order to identify day and night periods, we need to convert all timestamps into local time. To do so, we reverse-geocode the GPS coordinate of each measurement using OpenStreetMap's Nominatim [31] to determine the corresponding country. Then we convert the timestamp in UTC to a timestamp in the local timezone of the GPS coordinate using `timezonefinder` python library [32].

Identifying physical and logical WiFi sources. Identifying the physical sources of radio frequencies is particularly important for assessing exposure. This notion of physical source can be tricky. In this paper, a physical source is the source of a carrier signal, that is, the source of a signal at a specific frequency. For Bluetooth, 2G, 3G, and 4G, one detected signal corresponds to one physical source, but this is not the case for Wi-Fi.

A Wi-Fi access point usually has one or two physical sources of emission, but the signals we measure correspond to logical sources, and it is common to have multiple logical sources for one physical source. We can obtain the carrier signal frequency for each measured source, and one might argue that this information is enough to identify the physical sources. However, it is not the case, as different physical sources can use the same frequency. This is a common issue in Wi-Fi as the number of available frequencies (called channels) is limited, and the density of sources is high.

Wi-Fi networks are based on the notion of a service set, that is, the idea that logical networks can be layered on top of a physical network. Such logical networks are identified by a Service Set ID (SSID) (usually a human-readable string) associated with a Basic Service Set ID (BSSID), which is a 6-byte, internationally unique identifier usually derived from the MAC address of the access point. The strategy used to derive a BSSID from a MAC address depends on the equipment and administrator. We observed three strategies: the BSSID differs from the MAC address by the first byte, the last byte, or both the first and last bytes.

Therefore, the rule we apply to identify a physical source in a user scan is the following: if several Wi-Fi measurements report the same frequency and have the same BSSID (excluding the first and last bytes in the comparison), we associate them to the same physical source. In addition, as logical sources for the same physical source might report different RSSI (because the measurements might not be performed at the exact same time), we consider that the RSSI of the physical source is the maximum RSSI of all the associated logical sources for a given scan.

In the rest of this paper, all results we report for Wi-Fi are for physical sources.

Bluetooth scan synchronization. When counting the number of sources, it is important to use the concept of an atomic scan, that is, a scan that reflects the instantaneous exposure as measured by the smartphone. Cellular and Wi-Fi scans are atomic because the Android API returns all current sources in a single call or callback. However, this is not the case for Bluetooth. When we start a Bluetooth scan, the smartphone will perform a Bluetooth inquiry request and wait for an answer from devices in the vicinity [33]. Therefore, devices will reply one by one, usually within 15 seconds of the start of the scan.

The heuristic we use to attribute replying devices to an atomic scan is to group together all Bluetooth devices whose inter-arrival is less than 15 seconds.

In the rest of this paper, each time we count the number of Bluetooth devices, we count the number of devices in an atomic scan as defined in this section.

Mitigation of the cellular scans limited to the SIM operator. We have explained in the *Limitations* section that the cellular measurements only take into account the RSSI from the operator declared in the SIM card. This limitation results in a significant underestimation of the cellular exposure. To mitigate this issue, in each scan, we multiple the RSSI corresponding to a cellular measurement with the number of operators in the country in which the scan was performed.

2.3. Personal exposure definition and calculation

We define personal exposure as the received power from all the electromagnetic field sources on the radio frequency bands exposing humans. The received power is a function of the emitting power that is expressed in Equation (1) where P_r is the received power, P_e is the emitting power, K is a constant dependant on the emitting and receiving antennas' characteristics, d is the distance to the source, and f is the signal frequency [34]. We see in Equation (1) that distance plays an important role in personal exposure, as does signal frequency: higher frequency signals fade faster than lower ones.

$$P_r = K \left(\frac{1}{4\pi df} \right)^2 P_e \qquad (1)$$

The analysis we perform in this paper is based on three main calculation steps that we describe and justify in the following. i) First, for all computations based on an exposure scan (as defined in Materials and Methods), we consider the sum of the received power in Watt of all signals in this scan. Computing the sum is relevant because an exposure scan is atomic in terms of time, so it represents all the signals simultaneously exposing an individual. ii) Second, we average the exposure scans of each user per month. This gives a per-user monthly average exposure. The rationale of computing per-user monthly averages is to prevent users with a large number of measurements from biasing the monthly average. iii) Third, for each country, we group the per-user monthly average exposures. When a user has been in different countries for a given month, we compute one monthly average exposure per country. Then, we compute the mean of these per-user monthly average exposures to obtain a monthly average exposure per country. Finally, we obtain the yearly average exposure by computing the mean of the monthly average exposure per country. Computing the yearly average exposure this way avoids bias that could be introduced by months with a larger than average number of users.

2.4. *Data availability*

Upon publication, all data used in this paper will be available online for scientific exploitation. The data consists of timestamped measurements of RSSI for each of the five types of signals considered in this paper (Wi-Fi, Bluetooth, 2G, 3G, 4G). All user IDs have been anonymized (using a salted hash), and all GPS locations have been replaced by one of the 13 countries we consider. When required to preserve user anonymity, we provide aggregated data using pre-processing steps. For instance, we provide the identification of the unique physical sources using our own anonymous source counter. A detailed description of the format of the data will be available on the online publication site.

3. Results

3.1. *World-wide sustained growth of radio exposure is primarily driven by WiFi*

Table 2 shows the evolution of the total personal exposure in the 13 countries with the largest number of measurements (as discussed in Materials and Methods). We observe an overall trend of increased exposure across all countries from 2017 to 2020. To confirm this trend, we computed the Spearman correlation on the monthly average exposure to evaluate the relationship between time (months) and the monthly average exposure for each country. Table 3 shows a significant positive correlation between time and exposure for most countries.

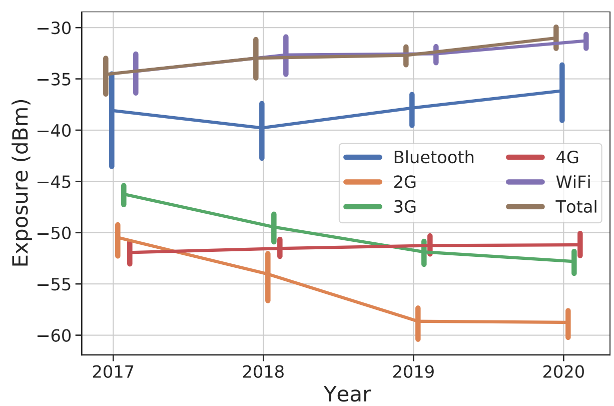

Figure 1: **The total exposure of the population has been multiplied by 2.3 in 4 years.** For each year, we take the yearly average exposure as given in Table 2, convert it to Watt, compute the mean for all 13 countries, and convert it back to dBm. The bars represent a 95% confidence interval for the mean using empirical bootstrap resampling with replacement (N=1,000) on the yearly average exposure per country. Plots are shifted horizontally to avoid confidence interval overlap. An increase of 3 dB results in the doubling of the exposure.

It is interesting to understand how each wireless technology contributes to this exposure trend. Figure 1 shows that the total exposure (brown curve) has been multiplied by 2.3 (from -34.6 dBm in 2017 to -31 dBm in 2020) over the four-year period. The trend

Country	2017 Mean	95%CI	2018 Mean	95%CI	Change	2019 Mean	95%CI	Change	2020 Mean	95%CI	Change
BR	-39.4	[-41.1, -38.1]	-36.3	[-39.1, -34.1]	+105%	-34.4	[-37.3, -32.4]	+56%	-32.0	[-33.1, -31.0]	+71%
AU	-34.2	[-37.4, -31.5]	-34.1	[-36.5, -32.1]	+2%	-31.0	[-34.0, -28.4]	+104%	-31.1	[-31.9, -30.4]	-3%
NL	-39.1	[-41.9, -36.9]	-37.1	[-39.6, -34.9]	+57%	-36.3	[-38.7, -34.3]	+19%	-33.6	[-35.3, -32.1]	+87%
IN	-29.8	[-35.1, -26.3]	-27.6	[-37.0, -23.6]	+64%	-32.2	[-33.8, -30.9]	-65%	-30.6	[-32.2, -29.4]	+46%
ES	-37.4	[-40.2, -35.1]	-35.4	[-37.6, -33.6]	+60%	-32.9	[-34.6, -31.7]	+77%	-31.6	[-32.9, -30.5]	+35%
BE	-40.7	[-42.0, -39.7]	-35.9	[-37.7, -34.3]	+204%	-35.4	[-36.5, -34.4]	+13%	-32.5	[-33.8, -31.5]	+91%
CH	-31.6	[-33.4, -30.2]	-32.9	[-34.4, -31.7]	-25%	-33.1	[-34.9, -31.6]	-6%	-32.6	[-34.3, -31.2]	+13%
GB	-39.2	[-41.0, -37.7]	-34.7	[-36.8, -32.9]	+182%	-32.7	[-35.1, -30.6]	+60%	-30.9	[-32.3, -29.8]	+49%
CA	-35.6	[-37.8, -33.8]	-32.3	[-33.5, -31.0]	+112%	-31.9	[-33.3, -30.6]	+9%	-29.2	[-30.1, -28.3]	+89%
DE	-36.6	[-37.5, -35.9]	-36.9	[-38.4, -35.8]	-7%	-32.8	[-34.8, -31.3]	+158%	-32.1	[-33.0, -31.0]	+19%
IT	-33.8	[-38.4, -30.7]	-33.9	[-35.3, -32.7]	-2%	-33.3	[-34.1, -32.4]	+16%	-32.1	[-33.1, -31.4]	+30%
US	-33.5	[-34.9, -32.0]	-30.5	[-31.2, -29.9]	+98%	-29.8	[-31.0, -28.5]	+18%	-27.3	[-28.3, -26.4]	+76%
FR	-33.5	[-34.1, -33.0]	-33.0	[-33.8, -32.2]	+14%	-33.3	[-33.9, -32.7]	-7%	-31.8	[-32.2, -31.4]	+42%

Table 2: **The yearly average exposure increased from 2017 to 2020 worldwide.** This table represents the evolution of the yearly average exposure per country. We use an ISO 3166 [35] alpha-2 country code to represent each country using a two-letter code. We compute the mean and the 95% confidence interval for the mean using empirical bootstrap resampling with replacement (N=1,000) [36] on the monthly average exposure for each country. The change column shows the increased (in blue) or decreased (in red) exposure as a percentage compared to the previous year. This percentage change is computed in Watt instead of dBm to have a linear interpretation of the change in exposure.

we observe for each wireless technology corresponds to the adoption or decline of the corresponding technology. We observe a clear increase in the exposure due to Wi-Fi and Bluetooth technologies, but a decrease in the exposure due to 2G and 3G technologies. Interestingly, Wi-Fi is by far the largest contributor to exposure.

In summary, we observe an overall increase in total personal exposure with time (a 2.3-fold increase from 2017 to 2020), with Wi-Fi being the largest contributor to personal exposure.

3.2. Exposure growth is not explained by the multiplication of sources

We focus now on how each source contributes to total exposure. This is a central question because an improved understanding of the most exposing sources could inform strategies for reducing personal exposure.

Since the measurement of the number of sources is not reliable for cellular technologies (see Materials and Methods), we focus on Wi-Fi and Bluetooth technologies. We consider this limitation reasonable because, as shown in Figure 1, these two are the most significant contributors to total exposure.

Table 3: **The Spearman correlation shows a significant positive correlation between time and exposure for most countries.** The Spearman correlation is computed on the monthly averages for each country from 01/2017 to 12/2019. We exclude 2020 from this correlation as the COVID-19 period would have significantly impacted the interpretation of this correlation. In blue, we show the positive correlations, and in red, the negative ones. The grey two-sided p-values are above the threshold of 0.05. When including 2020, we observe an increase in the Spearman coefficients between 0.1 and 0.2 for most countries and lower p-values for all countries (except CH), showing the impact of lockdowns on exposure. The most significant difference is France, with a Spearman coefficient of 0.42 (p<0.01).

country	BR	AU	NL	IN	ES	BE
score	0.44	0.45	0.37	0.14	0.42	0.63
p-value	0.0066	0.0058	0.026	0.4	0.011	3.4E-05
CH	GB	CA	DE	IT	US	FR
-0.21	0.7	0.57	0.47	0.36	0.62	0.00
0.23	2.2E-06	0.0003	0.0039	0.03	5.8E-05	0.99

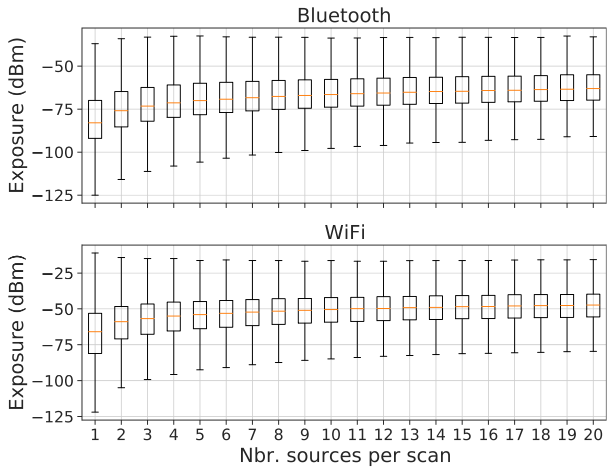

Figure 2: **A large number of sources in the vicinity marginally increases individual exposure.** The figure represents the distribution of all the exposure scans in Bluetooth (top) and Wi-Fi (bottom) when there is a given number of (Bluetooth or Wi-Fi) sources in the scan (the boxplot convention is the following: the middle orange line shows the median, the lower and higher hinges show the first and third quartiles, respectively, and the lower and higher whiskers show a limit of 1.5x the interquartile range from the lower and higher hinges, respectively). For instance, the last box in the top figure represents the sum of the received power in Bluetooth for exposure scans with exactly 20 detected Bluetooth sources. We observe that beyond 4 to 5 sources in the vicinity, any additional sources marginally change the individual exposure.

Figure 2 shows the relationship between individual exposure and the number of sources in a vicinity. We observe that beyond four to five sources, additional sources do not significantly increase individual exposure. Although this finding might seem counterintuitive, it is mainly explained by the important fading with the distance of the electromagnetic fields (see Equation 1). In addition, we see in Figure 3 that in 50% of the exposure scans, the most exposing Wi-Fi source (resp. Bluetooth) represents at least 83% (resp. 91%) of the total exposure due to Wi-Fi (resp. Bluetooth). Thus, the number of sources in the vicinity is not a good predictor of personal exposure; rather, the most exposing source is the primary contributor to exposure.

The question now is how actionable this information is with respect to exposure reduction. To answer, we focus on the Wi-Fi-connected sources and

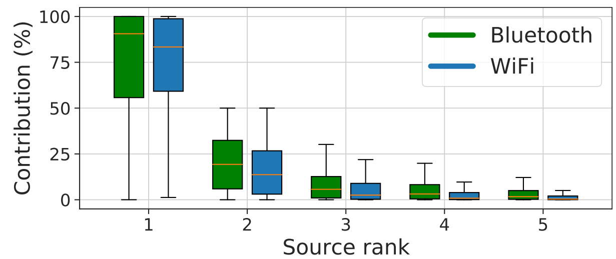

Figure 3: **The most exposing source is the primary driver of individual exposure.** This figure represents the distribution of the percentage contribution of the top five exposure sources in all exposure scans, with Bluetooth in green and Wi-Fi in blue (the boxplot convention is the following: the middle line shows the median, the lower and higher hinges show the first and third quartiles, respectively, and the lower and higher whiskers show a limit of 1.5x the interquartile range from the lower and higher hinges, respectively). For instance, the first green box shows the distribution of the contribution of the most exposing Bluetooth source to the sum of the exposure of all Bluetooth sources for each exposure scan. We observe that for 75% of the exposure scans (containing at least one Bluetooth measurement), the most exposing Bluetooth source represents at least 56% of the entire Bluetooth exposure.

Bluetooth-bounded devices to which a user has already connected. Connected sources or bounded devices are usually owned or controlled by the user and can therefore be switched off or moved to reduce exposure. Taking all scans into account, we computed that 41% of the time, the most exposing of all the Wi-Fi sources is a connected one. For Bluetooth, the most exposing source is a bounded device 10% of the time. Then, we computed what the individual personal exposure would have been if all connected sources and bounded devices had been switched off. While this is an overly optimistic situation, the goal is to assess the degree to which an individual could control exposure. Figure 4 shows that, by switching off the connected sources and bounded devices, half of the users could have reduced their total exposure by 50% (a reduction by 3.1 dB), and 25% could have reduced their total exposure by 90% (a reduction by 10 dB).

In summary, the growth of total exposure is not explained by a multiplication of sources. On the contrary, a handful of sources generate most of the personal exposure at any given time, and it is not uncom-

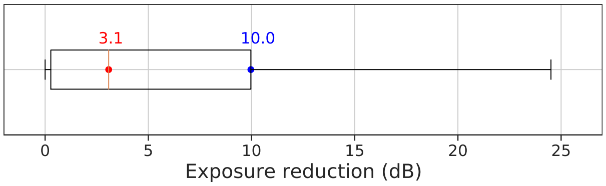

Figure 4: **By switching off connected Wi-Fi sources and bounded Bluetooth devices, 50% of the users can reduce their exposure by 3.1 dB, and 25% of the users can reduce it by at least 10 dB.** This figure shows the distribution of the individual exposure reduction for each user when we remove connected Wi-Fi sources and bounded Bluetooth devices. In red, we show the median and in blue, the 75^{th} percentile. For each user and month, we first compute the per-user monthly average exposure. Then, for each user and month, we collect all connected Wi-Fi sources and bounded Bluetooth devices, and we re-compute the per-user monthly average exposure by removing all collected connected sources and bounded devices from the exposure scans. Finally, we compute the difference between the per-user monthly average exposure in each case. The result is the distribution shown in this figure for each user. Note that in some rare cases, the difference can be negative. This can occur when an exposure scan contains only one connected source. By removing connected sources, we change the number of samples on which we average. As a result, a user with only a few samples could end up with a higher average without connected sources. In this figure, we drop users with a negative gain; they represent 0.92% of all users.

mon that an individual's exposure is almost entirely the result of sources they either own or associate with (for a quarter of our subjects, such sources account for 90% of exposure).

3.3. Impact of regulation on personal exposure

Electromagnetic field emissions are regulated, which means that both the spectrum used and the emitting power per frequency band are fixed by a regulatory authority. The types of cellular and Wi-Fi sources we explore in this paper are regulated on a country-specific basis. Therefore, the maximum emitting power per frequency band is not uniform in the top 13 countries we consider. By contrast, Bluetooth uses the same emitting power in all the countries we consider. We explore next how cellular and Wi-Fi regulation impacts the received power.

3.3.1. Cellular regulation

The maximum allowed exposure of the population is fixed by the ICNIRP international body [37]. However, each country is free to lower the maximum exposure depending on local policies. In addition, some countries have policies specific to some areas (e.g., Belgium has different limits for Flanders, Wallonia, and Brussels) or specific to some contexts (e.g., Italy enforces lower exposure near schools). Finally, the limits are specific to the frequencies used by cellular technologies. Here, we specifically focus on the frequencies 900 MHz, 1800 MHz, and 2100 MHz. For each country, we build a regulation limit triplet, one limit per frequency.

To the best of our knowledge, there is no central repository of exposure limits for all countries. To obtain a regulation limit triplet for each of the 13 countries we consider, we consolidated several sources [38, 39, 26], and when multiple limits were provided (due to local policies or context), we keep the limit covering the largest population.

Figure 5 does not show any clear correlation between regulation limits and exposure. We must be careful interpreting this result as there are several external factors that we do not control, such as the deployment strategy of the cellular operators. For example, operators might decide, in a densely populated area, to have a higher density of base stations (to increase the supported load) emitting at a lower power (to reduce interference). In such cases, base stations expose the population at a level that is significantly lower than what the regulation permits [26, 15]. Therefore, in practice, the regulation is an upper bound to the population exposure in some extreme cases, but in most cases, the population is exposed at levels much lower than the regulation limits.

To confirm this hypothesis, we computed the distribution of the cellular measurements in V/m. We obtain the electric field E in V/m from the measured received power in dBm with the formula:

$$E = \frac{9.73 f \sqrt{50 \times 10^{\frac{P-30}{10}}}}{c\sqrt{G}} \qquad (2)$$

where G is the antenna gain, f is the frequency in Hz,

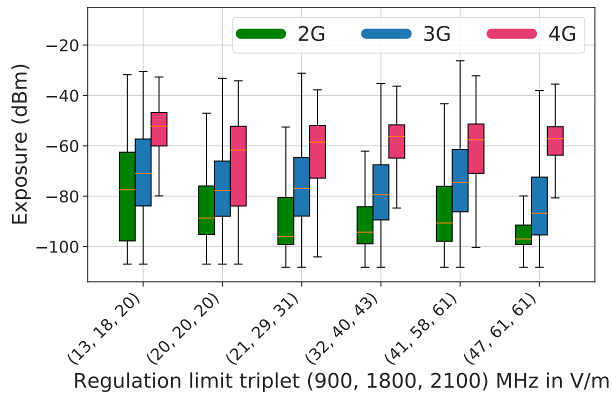

Figure 5: **We observe no correlation between regulation limits and exposure.** This figure shows the correlation between the exposure and a regulation limit triplet for the three cellular technologies we measure, 2G, 3G, and 4G (the boxplot convention is the following: the middle orange line shows the median, the lower and higher hinges show the first and third quartiles, respectively, and the lower and higher whiskers show a limit of 1.5x the interquartile range from the lower and higher hinges, respectively). Here is the association between regulation limit triplets and countries: (13, 18, 20) is for IN; (20, 20, 20) is for IT; (21, 29, 31) is for BE; (32, 40, 43) is for CA; (41, 58, 61) is for FR, DE, GB, CH, ES, NL, AU, BR; (47, 61, 61) is for US.

P is the power in dBm, and c is the speed of light [40]. The antenna gain of the smartphone is unknown, so we assume an isotropic antenna (i.e., $G = 1$). In our dataset, we have access to the cellular frequency f for serving cells only. Therefore, we only keep exposure scans with a serving cell containing a valid frequency (they represent 74.5% of all exposure scans). We sum all the cellular RSSI[2] in each exposure scan and convert the summed RSSI into V/m using the frequency of the serving cell.

Figure 6 shows the distribution of the measured electric field for each exposure scan per country. We see that the current population exposure is orders of magnitude lower than any current regulation limit. We found that by considering all countries together, only 1% of the scans are above 0.18 V/m.

[2]As explained in Materials and Methods, we perform the sum in Watt, and because we only measure the RSSI for the operator declared in the SIM card, we multiply each RSSI by the number of operators in the country in a pre-processing phase.

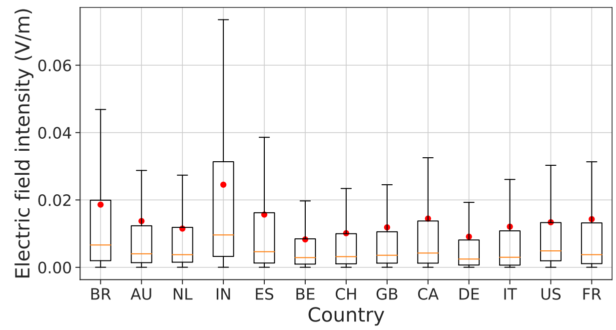

Figure 6: **The population exposure is orders of magnitude lower than any existing regulation limits for the considered countries.** This figure shows the distribution of the estimated electric field produced by cellular antennas at the receiver per country using boxplots, where the middle orange line shows the median, the lower and higher hinges show the first and third quartiles, respectively, and the lower and higher whiskers show a limit of 1.5x the interquartile range from the lower and higher hinges, respectively. The red dot shows the mean. Considering all signals together, we have a median at 0.005 V/m, and a 99$^{\text{th}}$ percentile at 0.18 V/m.

Admittedly, this estimation is a coarse description of reality. We now explore how the different limitations and approximations of our estimation will impact our conclusion. First, as described in Materials and Methods, the maximum cellular RSSI that we can measure is -51 dBm, so measurements above -51 dBm are capped. However, measurements at -51 dBm represent only 1.8% of all measurements, a very small fraction that cannot fundamentally change our conclusions. Second, we apply the same frequency (that of the serving cell) to all cellular measurements in the same exposure scan. Considering that 98% of the frequencies are within [782, 2660] MHz and Equation 2 is linear with f, we have at most a factor of 3.4. Note that this is a very conservative estimate, as the median frequency is 1,745 MHz. Last, in Boussad *et al.*[41], we show, using calibrated measurements in an anechoic chamber, that the average deviation between the real received power at a calibrated isotropic antenna and a smartphone is 2.5 dB. If we translate this offset in Equation 2, we find that it results in a multiplying factor of $\sqrt{10^{\frac{2.5}{10}}} \approx 1.3$. By combining the two main

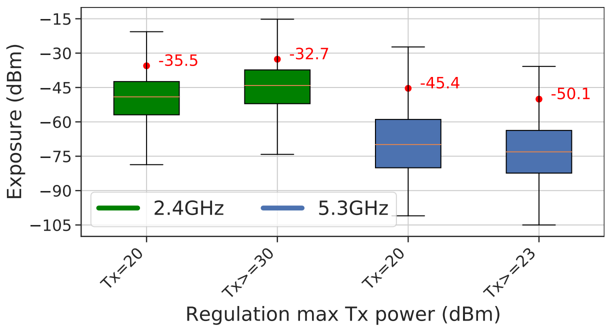

Figure 7: **The mean exposure is significantly higher when the Tx power is higher in the 2.4 GHz band, but significantly lower in the 5.3 GHz band.** The figure shows the distribution of the per-user monthly average exposure using boxplots. The middle orange line shows the median, the lower and higher hinges show the first and third quartiles, respectively, and the lower and higher whiskers show a limit of 1.5x the interquartile range from the lower and higher hinges, respectively. The red dot shows the mean. To compute the significance of the mean, we perform a permutation test (N=1,000,000). The test statistic is the difference of the means for the same frequency band. The two-sided p-value is lower than 0.001 for both bands.

sources of error, the actual exposure in V/m could be 4.4 times higher than what we report in Figure 6, which is still orders of magnitude lower than the most restrictive regulation limits in the countries we consider.

In summary, 99% of our exposure scans report a cellular exposure lower than 0.18 V/m (corrected to 0.79 V/m if we take into account the multiplying factor of 4.4, corresponding to a worst-case estimate scenario), which is orders of magnitude lower than any regulation limits in the considered countries.

3.3.2. WiFi regulation

Wi-Fi is a generic term that gathers together a large number of standards covering a wide spectrum of frequencies in the 2.4 GHz and 5 GHz bands. For Wi-Fi, the goal of regulation is to reduce interference by limiting the maximum transmission power. This limit might be different for each country and each frequency. Getting a consolidated view of the various international regulations on Wi-Fi is tricky. For this purpose, we rely on the efforts of J. W. Linville and S. Forshee, who maintain a consolidated file containing the Wi-Fi emitting power per country and frequency for the Linux kernel [42].

To understand the impact of regulation on exposure, we focus on two frequency bands that include a large enough number of countries using different regulations: 2.4 GHz ([2400, 2483] MHz) and 5.3 GHz ([5250, 5350] MHz). The 2.4 GHz (resp. 5.3 GHz) band represents 76% (resp. 2%, still 37 million measurements) of all Wi-Fi measurements. In the 2.4 GHz band, the maximum transmission power is 36 dBm for Australia, 30 dBm for the USA and Canada, and 20 dBm for all the other considered countries. In the 5.3 GHz band, the maximum transmission power is 24 dBm for Brazil, India, and Canada, 23 dBm for the USA, and 20 dBm for all the other considered countries.

Figure 7 shows that in the 2.4 GHz band, a Tx power of 20 dBm leads to significantly lower exposure than a Tx power higher than 30 dBm. Therefore, this regulation clearly impacts population exposure. Surprisingly, when we observe the exposure for the 5.3 GHz band, we have the opposite result: a Tx power of 20 dBm leads to significantly higher exposure than a Tx power over 23 dBm.

We can explain this seemingly contradictory result. Unlike regulations for cellular, regulations for Wi-Fi limit the Tx power; therefore, it is not surprising to see that Tx power impacts population exposure. When the difference in Tx power is large (a minimum of 10 dB between the two groups in the 2.4 GHz band), the Tx power dominates the other factors that affect population exposure. However, when the difference in the Tx power is small (a maximum of 4 dB for the 5.3 GHz band), other factors dominate the population's exposure. Indeed, as the attenuation increases with the frequency (see Equation 1), a small 4 dB difference in the Tx power will have a marginal impact on the total exposure compared to, for instance, the deployment and density of Wi-Fi access points per country.

In summary, the impact of Wi-Fi regulation on population exposure depends not only on the Tx power, but also on the frequency bands. It is worth noting that the goal of this regulation is to limit interference rather than population exposure.

3.4. *The population is most exposed at home*

User location is also a factor that may affect personal exposure. In the following, we focus on two location categories: at-home and out-of-home. The rationale is that, according to the results reported in the previous sections, Wi-Fi is the greatest contributor to total exposure. We hypothesize that users are more exposed at home because most users have Wi-Fi at home[3] and are closer to their router than would be the case in other environments. The goal of this section is to explore the difference between at-home and out-of-home exposure.

To cluster measurements according to the user location, we need users with a large enough number of measurements to identify the home location; we call them *dense users*. More precisely, when we compute the per-user monthly average exposure, we only keep users with at least 14 days of data in that month and at least 80% hourly sampling density. To calculate sampling density, we count the number of hours between the first and last day we see a user in a given month. An 80% hourly sampling density means that the user has at least one exposure scan for 80% of the counted hours. In our entire dataset, we have 22,907 dense users, which is 9% of all users.

Finally, we use the DBSCAN algorithm [45] (ϵ = 100 meters, minPts = 24, distance = haversine) on the GPS coordinates of the dense users for each month, independently. We label the cluster that most frequently appears between 10PM and 8AM as the home cluster. All the other clusters are labeled "out-of-home". Therefore, out-of-home gathers together all other indoor and outdoor locations, including those frequented for work, transportation, etc.

Figure 8 shows that users at home are significantly less exposed to cellular radiation. The main reason is that cellular antennas are outside, so walls attenuate the radiation. Conversely, exposure to Wi-Fi is more important at home than out-of-home. Here, the increased adoption of Wi-Fi technology at home

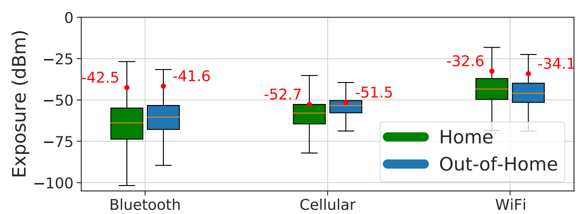

Figure 8: **The mean exposure is significantly lower at home for cellular (-1.19 dB) and higher at home for Wi-Fi (+1.55 dB).** This figure shows the distribution of the per-user monthly average exposure for dense users when they are at home (in green) and out-of-home (in blue) for Bluetooth, Cellular, and Wi-Fi sources. In the boxplots, the middle orange line shows the median, the lower and higher hinges show the first and third quartiles, respectively, and the lower and higher whiskers show a limit of 1.5x the interquartile range from the lower and higher hinges, respectively. The red dots and labels show the mean exposure. We performed a permutation test (N=1,000,000) between at-home and out-of-home for each of the three types of sources. We obtained a two-sided $p < 0.001$ for Wi-Fi and Cellular, and a two-sided $p = 0.09$ for Bluetooth.

is a reasonable explanation. We computed how many hours (per month) each dense user is connected to a Wi-Fi source at home and out-of-home. We found that half of the users (median) are connected 91% of the time at home, and 29% of the time out-of-home. Finally, we found that the difference of exposure to Bluetooth between at-home and out-of-home is not significant.

In summary, user location has a significant impact on exposure. In particular, users are more exposed to Wi-Fi at home. As they are largely connected to Wi-Fi at home, we further conclude that personal Wi-Fi routers are the most significant factor in at-home exposure.

4. Discussion

Understanding the potential human health impacts of exposure to radio frequencies is a long journey. An important challenge in performing sound epidemiological studies is the complexity of characterizing the real exposure of the population. The methods and dataset we present here offer the first analysis of the

[3]According to the US Census Bureau, 81% of USA households had internet access in 2016 [43]. In 2019, more than 80% of the households in the European countries included in our study had internet access, with 83% coverage in France and 98% in the Netherlands) [44].

evolution of radio frequency exposure at population-scale for 13 countries over four years. This change of paradigm from previous small-scale studies has direct consequences for the current debate on population exposure and the impact of this exposure on health.

The Council of Europe, following the principle of precaution, has called for an *As Low As Reasonably Achievable* (ALARA) rule [46]. In line with this principle, one proposal is to reduce exposure levels as low as 0.6 V/m and even 0.2 V/m in the medium term. The debate currently includes proponents, who see ALARA as a necessary drastic reduction to curb the current level of exposure, and cellular operators, who oppose ALARA by arguing that it would impede the deployment of communication infrastructure, and thus, eventually, access. We reveal that for the vast majority of the population, exposure is already below the lowest ALARA level. However, reducing the current regulation levels would still benefit the small fraction of the population that is currently more exposed than recommended by the ALARA rule.

Our work also fundamentally changes the debate on frequency exposure, currently heavily centered on the regulation of cellular operators. Not only do we show that Wi-Fi is by far the largest contributor to population exposure, but also that a few sets of sources, namely those used by individuals and those present at home, are the key contributors. Offering tools for individuals to prevent unnecessary exposure at home, or working on technology that automatically reduces exposure are just some examples of short and medium term ways to expand the precautionary principle. Such approaches have not yet received the attention that they deserve.

Beyond these direct implications, we envision our work and dataset providing a foundation for future epidemiological studies.

CRediT authorship contribution statement

Y. Boussad: Conceptualization, Data curation, Formal Analysis, Investigation, Methodology, Software, Validation, Visualization, Writing original draft, Writing review & editing. **X. Chen:** Formal Analysis, Methodology, Software, Validation, Visualization, Writing original draft, Writing review & editing. **A. Legout:** Conceptualization, Data curation, Formal Analysis, Funding acquisition, Investigation, Methodology, Project administration, Resources, Software, Supervision, Validation, Writing original draft, Writing review & editing. **A. Chaintreau:** Conceptualization, Formal Analysis, Methodology, Resources, Supervision, Validation, Writing original draft, Writing review & editing. **W. Dabbous:** Writing original draft, Writing review & editing.

Conflicts of Interest:

The authors declare no conflict of interest.

5. Acknowledgement

The authors wish to thank Sandra Matz for feedback on this work, as well as Mondi Ravi and David Migliacci for their central work on the ElectroSmart app.

This work has been supported by the French government, through the UCAJEDI Investments in the Future project managed by the National Research Agency (ANR) with the reference number ANR-15-IDEX-01.

References

[1] S. Gupta, R. S. Sharma, R. Singh, Non-ionizing radiation as possible carcinogen, International Journal of Environmental Health Research 1 (2020) 1–25. 0ondoi:10.1080/09603123.2020.1806212.

[2] J. W. Frank, Electromagnetic fields, 5G and health: what about the precautionary principle?, J. Epidemiol. Community Health jech-2019-213595. 0onarXiv:33468601, 0ondoi:10.1136/jech-2019-213595.

[3] L. Hardell, World Health Organization, radiofrequency radiation and health - a hard nut to crack (Review), Int. J. Oncol. 51 (2) (2017) 405–413. 0ondoi:10.3892/ijo.2017.4046.

[4] T. Saliev, D. Begimbetova, A.-R. Masoud, B. Matkarimov, Biological effects of non-ionizing electromagnetic fields: Two sides of a coin, Prog. Biophys. Mol. Biol. 141 (2019) 25–36. 0ondoi:10.1016/j.pbiomolbio.2018.07.009.

[5] J.-H. Moon, Health effects of electromagnetic fields on children, Clin. Exp. Pediatr. 63 (11) (2020) 422. 0ondoi:10.3345/cep.2019.01494.

[6] A. Di Ciaula, Towards 5G communication systems: Are there health implications?, Int. J. Hyg. Environ. Health 221 (3) (2018) 367–375. 0ondoi:10.1016/j.ijheh.2018.01.011.

[7] Electrosmart, [Online; accessed 1. Dec. 2020] (Jan. 2020).
URL 0onhttps://electrosmart.app

[8] I. A. for Research on Cancer, et al., Iarc classifies radiofrequency electromagnetic fields as possibly carcinogenic to humans, Press release 208.

[9] Standard IARC classification Glossary., [Online; accessed 18 May 2021] (May 2021).
URL 0onhttps://ec.europa.eu/health/scientific_committees/opinions_layman/en/electromagnetic-fields/glossary/ghi/iarc-classification.htm

[10] S. Sagar, S. M. Adem, B. Struchen, S. P. Loughran, M. E. Brunjes, L. Arangua, M. A. Dalvie, R. J. Croft, M. Jerrett, J. M. Moskowitz, et al., Comparison of radiofrequency electromagnetic field exposure levels in different everyday microenvironments in an international context, Environment international 114 (2018) 297–306.

[11] M. Velghe, W. Joseph, S. Debouvere, R. Aminzadeh, L. Martens, A. Thielens, Characterisation of spatial and temporal variability of rf-emf exposure levels in urban environments in flanders, belgium, Environmental research 175 (2019) 351–366.

[12] M. Eeftens, B. Struchen, L. E. Birks, E. Cardis, M. Estarlich, M. F. Fernandez, P. Gajšek, M. Gallastegi, A. Huss, L. Kheifets, et al., Personal exposure to radio-frequency electromagnetic fields in europe: Is there a generation gap?, Environment international 121 (2018) 216–226.

[13] S. Sagar, S. Dongus, A. Schoeni, K. Roser, M. Eeftens, B. Struchen, M. Foerster, N. Meier, S. Adem, M. Röösli, Radiofrequency electromagnetic field exposure in everyday microenvironments in europe: A systematic literature review, Journal of exposure science & environmental epidemiology 28 (2) (2018) 147–160.

[14] C. R. Bhatt, M. Redmayne, B. Billah, M. J. Abramson, G. Benke, Radiofrequency-electromagnetic field exposures in kindergarten children, Journal of exposure science & environmental epidemiology 27 (5) (2017) 497–504.

[15] D. Urbinello, W. Joseph, L. Verloock, L. Martens, M. Röösli, Temporal trends of radio-frequency electromagnetic field (RF-EMF) exposure in everyday environments across European cities, Environ. Res. 134 (2014) 134–142. 0ondoi:10.1016/j.envres.2014.07.003.

[16] R. Ramirez-Vazquez, J. Gonzalez-Rubio, E. Arribas, A. Najera, Characterisation of personal exposure to environmental radiofrequency electromagnetic fields in albacete (spain) and assessment of risk perception, Environmental research 172 (2019) 109–116.

[17] C. R. Bhatt, M. Redmayne, M. J. Abramson, M. R. Sim, C. Brzozek, B. M. Zeleke, G. Benke, Estimating transmitted power density from mobile phone: an epidemiological pilot study with a software modified phone, Australasian physical & engineering sciences in medicine 41 (4) (2018) 985–991.

[18] R. Ramirez-Vazquez, J. Gonzalez-Rubio, I. Escobar, C. d. P. Suarez Rodriguez, E. Arribas, Personal exposure assessment to wi-fi radiofrequency electromagnetic fields in mexican microenvironments, International Journal of Environmental Research and Public Health 18 (4) (2021) 1857.

[19] L. E. Birks, B. Struchen, M. Eeftens, L. van Wel, A. Huss, P. Gajšek, L. Kheifets, M. Gallastegi, A. Dalmau-Bueno, M. Estarlich, et al., Spatial and temporal variability of personal environmental exposure to radio frequency electromagnetic fields in children in europe, Environment international 117 (2018) 204–214.

[20] M. Gallastegi, A. Huss, L. Santa-Marina, J. J. Aurrekoetxea, M. Guxens, L. E. Birks, J. Ibarluzea, D. Guerra, M. Röösli, A. Jiménez-Zabala, Children's exposure assessment of radiofrequency fields: Comparison between spot and personal measurements, Environment international 118 (2018) 60–69.

[21] S. Aerts, J. Wiart, L. Martens, W. Joseph, Assessment of long-term spatio-temporal radiofrequency electromagnetic field exposure, Environmental research 161 (2018) 136–143.

[22] J. Breckenkamp, M. Blettner, J. Schüz, C. Bornkessel, S. Schmiedel, B. Schlehofer, G. Berg-Beckhoff, Residential characteristics and radiofrequency electromagnetic field exposures from bedroom measurements in Germany, Radiat. Environ. Biophys. 51 (1) (2012) 85–92. 0onarXiv:21964673, 0ondoi:10.1007/s00411-011-0389-2.

[23] S. Sagar, S. Dongus, A. Schoeni, K. Roser, M. Eeftens, B. Struchen, M. Foerster, N. Meier, S. Adem, M. Röösli, Radiofrequency electromagnetic field exposure in everyday microenvironments in Europe: A systematic literature review, J. Exposure Sci. Environ. Epidemiol. 28 (2018) 147–160. 0ondoi:10.1038/jes.2017.13.

[24] A. Lahham, H. Ayyad, Personal exposure to radiofrequency electromagnetic fields among palestinian adults, Health physics 117 (4) (2019) 396–402.

[25] B. M. Zeleke, C. Brzozek, C. R. Bhatt, M. J. Abramson, R. J. Croft, F. Freudenstein, P. Wiedemann, G. Benke, Personal exposure to radio frequency electromagnetic fields among australian adults, International journal of environmental research and public health 15 (10) (2018) 2234.

[26] D. Urbinello, W. Joseph, A. Huss, L. Verloock, J. Beekhuizen, R. Vermeulen, L. Martens, M. Röösli, Radio-frequency electromagnetic field (rf-emf) exposure levels in different european outdoor urban environments in comparison with regulatory limits, Environment international 68 (2014) 49–54.

[27] Operational Committee for the assesment of Legal and Ethical risks., [Online; accessed 18 May 2021] (May 2021).
URL 0onhttps://www.inria.fr/en/operational-committee-assesment-legal-and-ethical-risks

[28] European general data protection regulation (gdpr), [Online; accessed 1. Dec. 2020] (Dec. 2020).
URL 0onhttps://gdpr-info.eu/

[29] T. Mazloum, A. Danjou, J. Schûz, S. Bories, A. Huss, E. Conil, I. Deltour, J. Wiart, Xmobisenseplus: An updated application for the assessment of human exposure to rf-emfs, in: 2020 XXXIIIrd General Assembly and Scientific Symposium of the International Union of Radio Science, 2020, pp. 1–2. 0ondoi:10.23919/URSIGASS49373.2020.9232310.

[30] Wikipedia: Exynos, [Online; accessed 1. Dec. 2020] (Dec. 2020).
URL 0onhttps://en.wikipedia.org/wiki/Exynos/

[31] OpenStreetMap Nominatim, [Online; accessed 15. Jan. 2021] (Jan. 2021).
URL 0onhttps://nominatim.openstreetmap.org/ui/search.html

[32] timezonefinder, [Online; accessed 15. Jan. 2021] (Jan. 2021).
URL 0onhttps://pypi.org/project/timezonefinder

[33] G. Chakraborty, K. Naik, D. Chakraborty, N. Shiratori, D. Wei, Analysis of the bluetooth device discovery protocol, Wirel. Netw. 16 (2) (2010) 421436. 0ondoi:10.1007/s11276-008-0142-1. URL 0onhttps://doi.org/10.1007/s11276-008-0142-1

[34] H. T. Friis, A Note on a Simple Transmission Formula, Proc. IRE 34 (5) (1946) 254–256. 0ondoi:10.1109/JRPROC.1946.234568.

[35] ISO 3166 Country Codes, [Online; accessed 16. Jun. 2021] (Jun 2021). URL 0onhttps://www.iso.org/iso-3166-country-codes.html

[36] B. Efron, R. J. Tibshirani, An introduction to the bootstrap, CRC press, 1994.

[37] ICNIRP, ICNIRP Guidelines on Limiting Exposure to Electromagnetic Fields, [Online; accessed 16. Jun. 2021] (2020). URL 0onhttps://www.icnirp.org/en/activities/news/news-article/rf-guidelines-2020-published.html

[38] WHO - Global Health Observatory data repository, Exposure limits for radio-frequency fields (public) data by country, [Online; accessed 22-February-2021] (2017). URL 0onhttps://apps.who.int/gho/data/view.main.EMFLIMITSPUBCRADIOFREQUENCYv

[39] Rianne Stam, National Institute for Public Health and the Environment, The Netherlands, Comparison of international policies on electromagnetic fields, [Online; accessed 22-February-2021] (2017). URL 0onhttps://mronline.org/wp-content/uploads/2020/05/Comparison20of20international20policies20on20electromagnetic20fields202018.pdf

[40] S. Y. Liao, Measurements and computations of electric field intensity and power density, IEEE Transactions on Instrumentation and Measurement 26 (1) (1977) 53–57.

[41] Y. Boussad, M. N. Mahfoudi, A. Legout, L. Lizzi, F. Ferrero, W. Dabbous, Evaluating smartphone accuracy for rssi measurements, IEEE Transactions on Instrumentation and Measurement 70 (2021) 1–12. 0ondoi:10.1109/TIM.2020.3048776.

[42] Wireless regulatory database for CRDA, [Online; accessed 8. Feb. 2021] (Feb. 2021). URL 0onhttps://git.kernel.org/pub/scm/linux/kernel/git/sforshee/wireless-regdb.git/about

[43] U. C. Bureau, Computer and Internet Use in the United States: 2016, United States Census Bureau 1. URL 0onhttps://www.census.gov/library/publications/2018/acs/acs-39.html

[44] Statistics | Eurostat, [Online; accessed 15. Sep. 2020] (Sep. 2020). URL 0onhttps://ec.europa.eu/eurostat/databrowser/view/tin00073/default/table?lang=en

[45] M. Ester, H.-P. Kriegel, J. Sander, X. Xu, et al., A density-based algorithm for discovering clusters in large spatial databases with noise., in: Kdd, Vol. 96, 1996, pp. 226–231.

[46] P. Assembly, The potential dangers of electromagnetic fields and their effect on the environment, no. Resolution 1815 (2011), Council of Europe, 2011. URL 0onhttp://assembly.coe.int/nw/xml/XRef/Xref-XML2HTML-en.asp?fileid=17994